

·Supplementary Material for

One-Pot Hydrothermal Synthesis of High Quantum Yield Orange-Emitting Carbon Quantum Dots for Sensitive Detection of Perfluorinated Compounds

Yushuang Hong^{a,†}, Xianping Chen^{a,†}, Ya Zhang^a, Yulin Zhu^a, Jingfang Sun^b, Mark T. Swihart^{c,}, Kejun Tan^{a,*} and Lin Dong^b*

^aKey Laboratory of Luminescence analysis and Molecular Sensing, Ministry of Education, College of Chemistry and Chemical Engineering, Southwest University, Chongqing 400715, China. E-mail: tankj@swu.edu.cn.

^b*School of the Environment, Jiangsu Key Laboratory of Vehicle Emissions Control, Center of Modern Analysis, School of Chemistry and Chemical Engineering, Nanjing University, Nanjing, 210093, P. R. China.*

^cDepartment of Chemical and Biological Engineering, The University at Buffalo, The State University of New York, Buffalo, New York 14260-4200, United States. E-mail: swihart@buffalo.edu.

[+] These authors contributed equally to this work.

Experimental

Apparatus

The UV absorbance and FL (FL) spectra of CQDs were obtained using UV-2600 (Shimadzu, Japan) and F-2700 spectrophotometers (Hitachi, Japan), respectively. The HRTEM images of CQDs were obtained with a Tecnai G2 F20 field emission transmission electron microscope (FEI, USA). The elements and functional groups of CQDs were recorded through an ESCALAB 250 X-ray photoelectron spectrometer and a Shimadzu FTIR-8400S spectrometer (Kyoto, Japan). The Raman spectrum of CQDs was recorded with a Lab RAM HR800 Laser confocal Raman spectrometer (Horiba Jobin Yvon, France) on the AgNP dispersion. The FL lifetime of CQDs was collected with an FL-TCSPC FL spectrophotometer (Horiba Jobin Yvon, France). The x-ray diffraction (XRD) pattern of CQDs was measured with a Rigaku Ultima IV instrument (Tokyo, Japan). FL imaging of CQDs was conducted on a DSU live-cell confocal microscope system (Olympus, Japan). Cyclic voltammograms were measured on a CHI 660E electrochemical workstation (CH Instruments, Shanghai, China). Zeta potentials of CQDs in different pH solutions were determined through a ZEN3600 dynamic laser light scattering (Malvern, English).

2.3 Biocompatibility of the obtained CQDs

The cytotoxicity of CQDs to Hep-2 cells was evaluated by a standard CKK-8 assay. Hep-2 cells ($1 \times 10^5 \text{ mL}^{-1}$) in Roswell Park Memorial Institute

1640 medium (RPMI 1640) supplemented with 10% fetal bovine serum (FBS) were added to each well of a 96-well plate (100 μL well⁻¹). Plates were first maintained in an incubator (37 °C, 5% CO₂) for 24 h. Then the culture medium was replaced with 2% FBS 1640 medium containing the CQDs at different concentrations (0, 10, 20, 40, 60, 80, 100 $\mu\text{g}/\text{mL}$) for another 24 h. Finally, 10 μL of Cell Counting Kit-8 (CCK-8) solution and 90 μL RPMI 1640 were added to each. The optical density (OD) of the mixture at 450 nm was measured with a microplate reader 30 minutes after CCK-8 solution addition. The cell viability was estimated according to the following equation:

$$\text{Cell Viability}(\%) = \frac{OD_{\text{treated}}}{OD_{\text{control}}} \times 100\%$$

2.4 Cell fluorescence imaging

Hep-2 cells in RPMI 1640 supplemented with 2% fetal bovine serum were added to imaging dishes (1 mL well⁻¹). The cells were first cultured in an incubator (37 °C, 5% CO₂) overnight, then 1 mL culture medium containing CQDs (20 $\mu\text{g}/\text{mL}$) was added to each dish and incubated for 2 h. The fluorescence images were acquired by a DSU live-cell confocal microscope (Olympus, Japan) system with laser excitation in the DAPI channel (350-370 nm), GFP channel (470-490 nm) and Cy3 channel (510-560 nm).

Pretreatment of actual sample

The samples were firstly heated to a boil, then cooled down and filtered using a 0.22 μm membrane. Then cation exchange resin was used to remove cation. The pretreated water samples were analyzed according to the experimental procedure of

PFOS/PFOA detection.

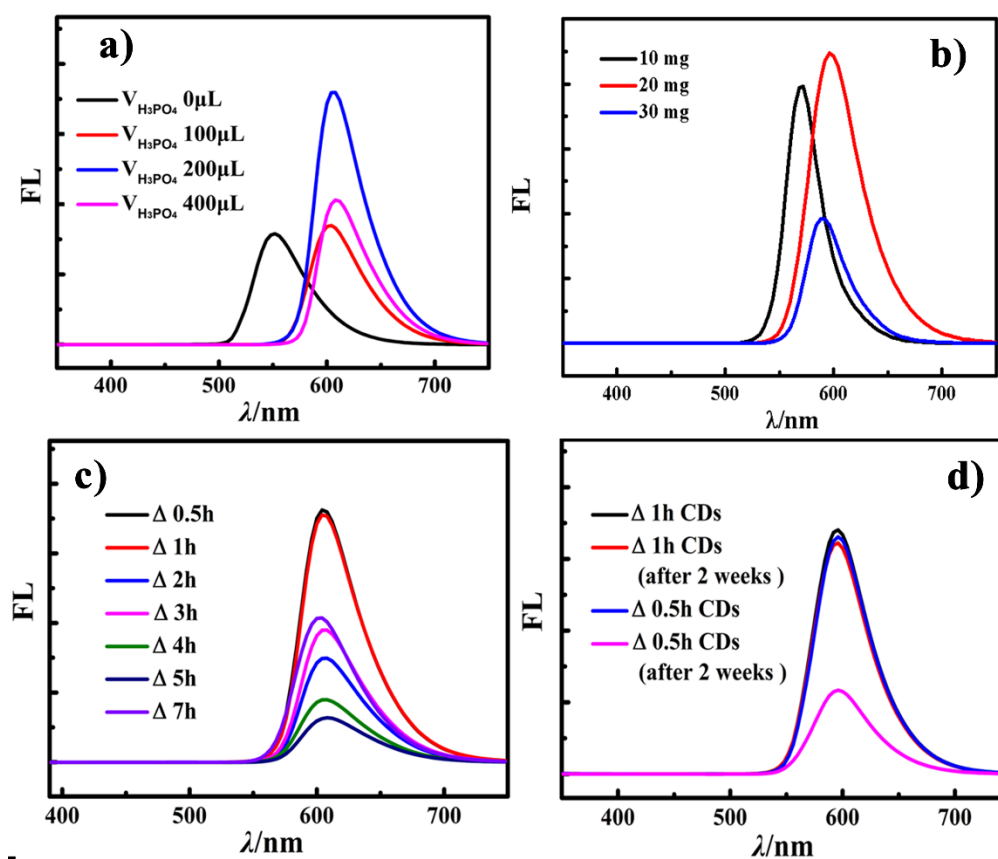


Fig. S1 Experiments for optimization of phosphoric acid content (a), the quality of 4- (diethylamino) salicylaldehyde (b), and reaction time (c,d) at 200 °C.

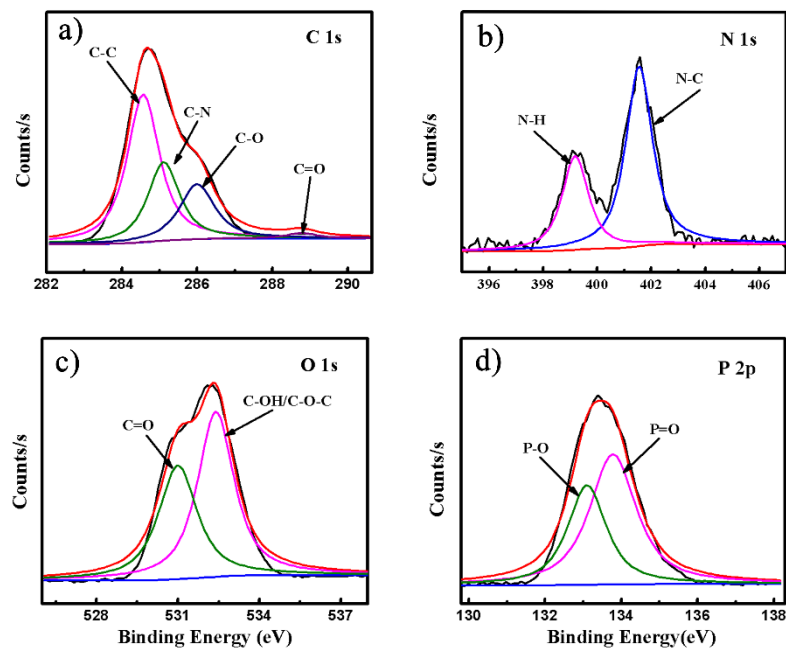


Fig. S2 XPS of CQDs: High-resolution spectra in the C 1s (a) N 1s (b) O 1s (c) and P 2p (d) regions

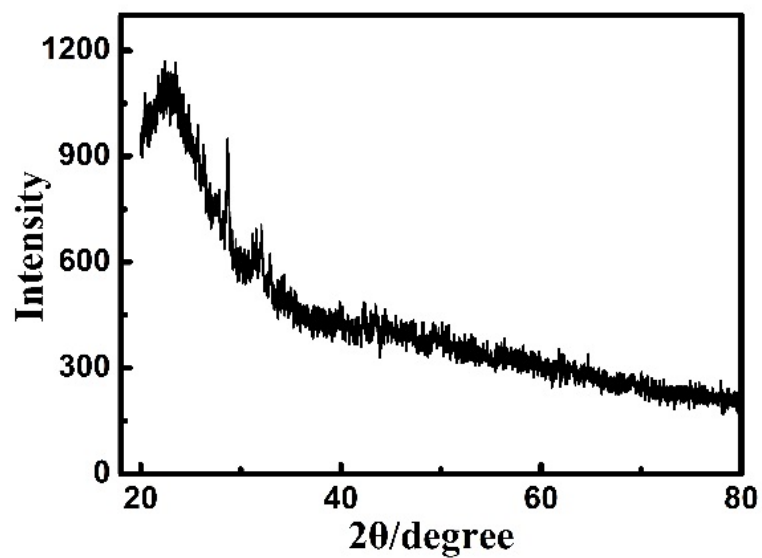


Fig. S3 XRD pattern of CQDs

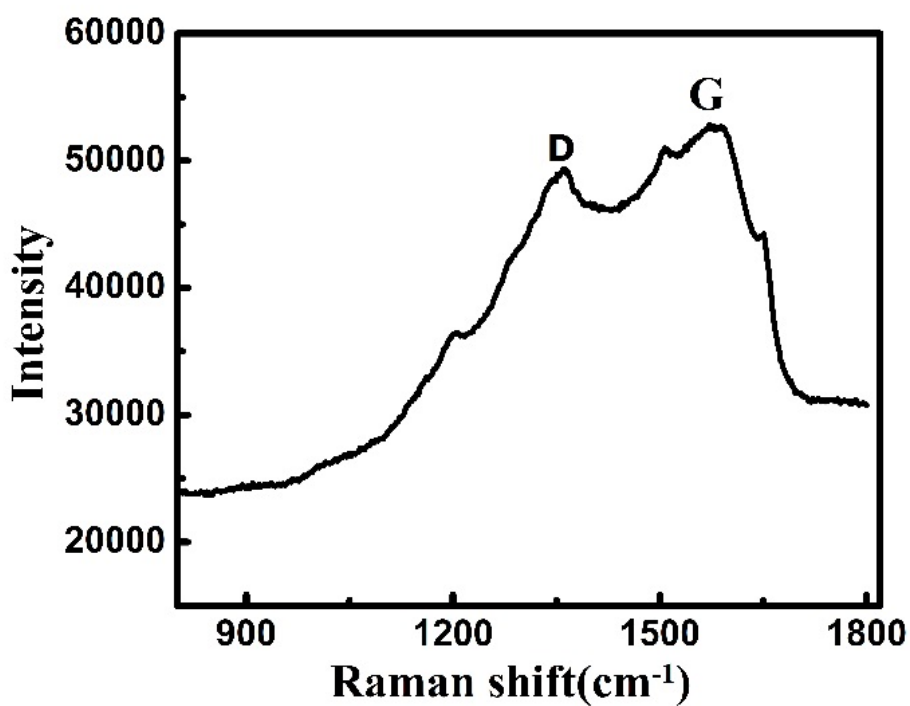


Fig. S4 Raman spectrum of CQDs

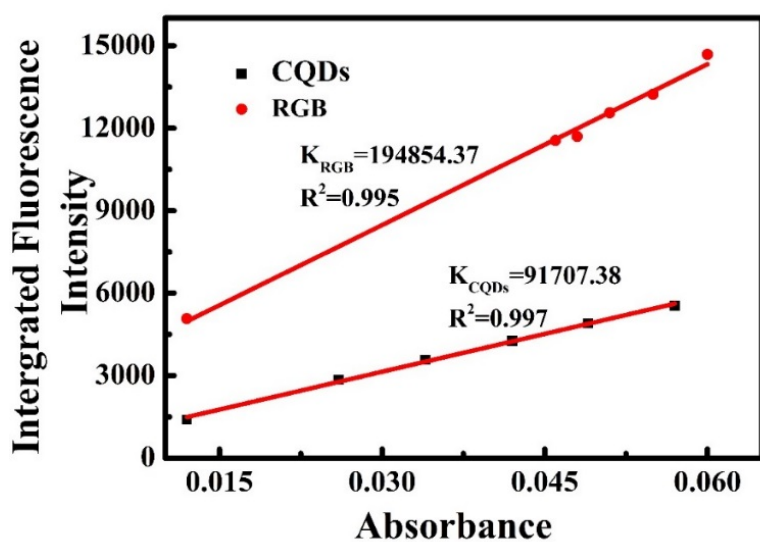


Fig. S5 Linear fitting for quantum yield calculation of CQDs and RGB

The QY was calculated according to the following formula:

$$Q_{CQDs} = Q_R \cdot \frac{I_{CQDs}}{I_R} \cdot \frac{A_R}{A_{CQDs}}$$

In this equation, Q is the quantum yield of our sample and I is the measured fluorescence intensity. A is the optical density at the excitation wavelength. QY was measured using Rhodamine B in ethanol (quantum yield is 0.98 at 550 nm) as a standard reference. The subscript “R” refers to the standard sample with known quantum yield and “CQDs” stands for the sample being tested. To minimize re-absorption effects, the absorbance of CQDs dispersion in a 10 mm fluorescence cuvette was kept ≤ 0.08 at the excitation wavelength of 550 nm. The QY obtained in this way for the sample presented in Fig. S5 was 47.1%.

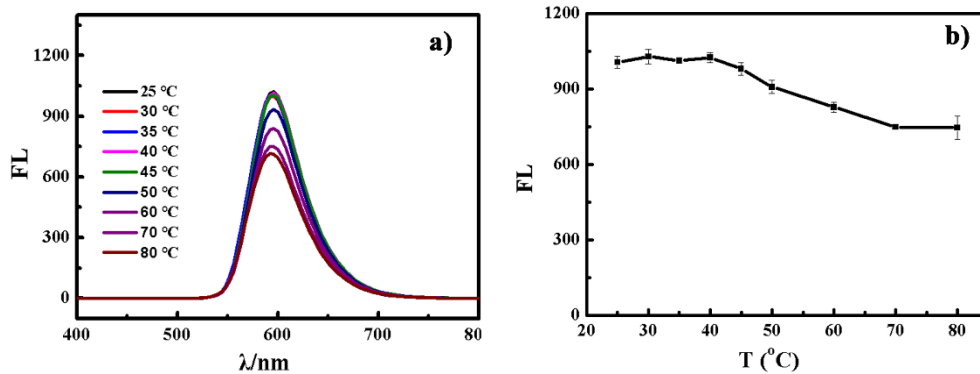


Fig. S6 (a) Fluorescence spectra of CQDs at temperatures from 25 to 80 °C. In both panels, intensity is in arbitrary units, but at fixed conditions other than temperature. Panel (b) plots the maximum intensity at a function of temperature

Table S1. Comparison of different methods for PFOS/PFOA sensing.

Method	Determinand	Linear range (μM)	LOD (nM)	References
UV-vis	PFOS	0.070-3.0	14.9	[1]
FL	PFOS	0.10-1.5	28.0	[2]
FL	PFOS	0.22-50	21.7	[3]
FL	PFOS	0-2.0	27.8	[4]
FL	PFOS	0.050-16	8.0	[5]
FL	PFOS	0.0050-2.0	1.0	[6]
FL	PFOA	10-70	1.8×10^3	[7]
FL	PFOA	0.50-40	3.0×10^2	[8]
FL	PFOA	0.050-10	11.8	[9]
FL	PFOA	0.25-15	25.0	[10]
FL	PFOS	0.050-1.0	5.0	This work
FL	PFOA	0.10-1.5	10.0	This work

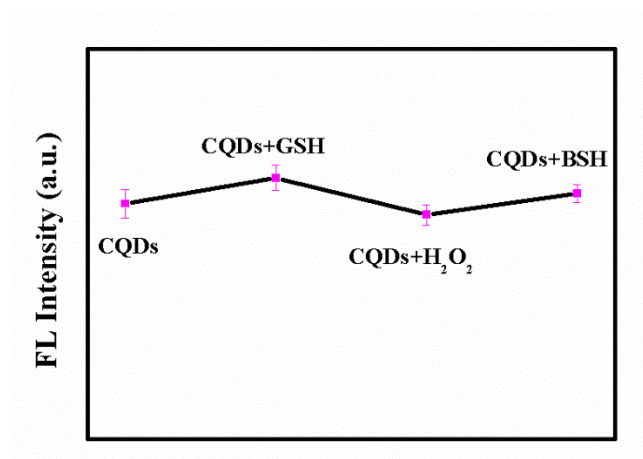


Fig. S7 FL stability of CQDs in different biological media.

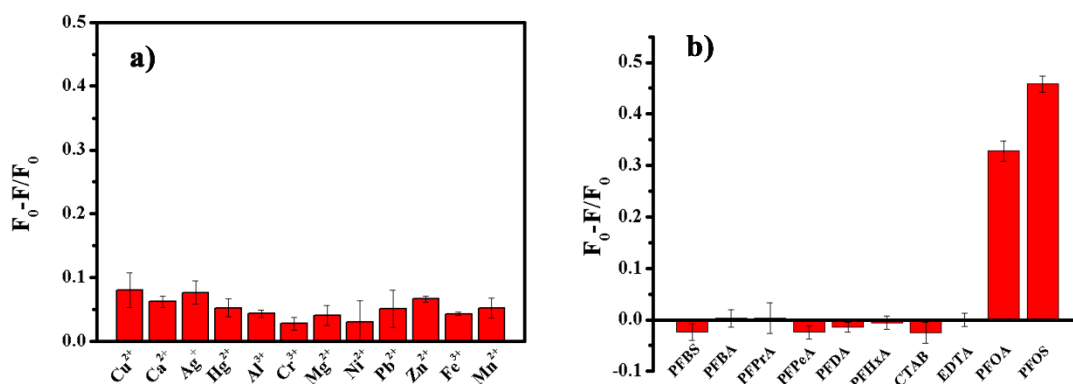


Fig. S8 Selective FL quenching of CQDs. FL responses of CQDs with (a) various metal ions at 1 μM concentration, (b) PFCs and some surfactants at 1 μM concentration. Excitation was at 560 nm, and emission was measured at 596 nm

The fluorescence intensity of CQDs remains stable from 25 $^{\circ}\text{C}$ to 45 $^{\circ}\text{C}$, then quenches to some degree as the temperature rises further. Increased molecular motion at higher temperature promotes energy transfer from the excited state to molecular vibrations and other motions, which increases the probability of return to the ground state via non-radiative paths, decreasing the fluorescence intensity[11].

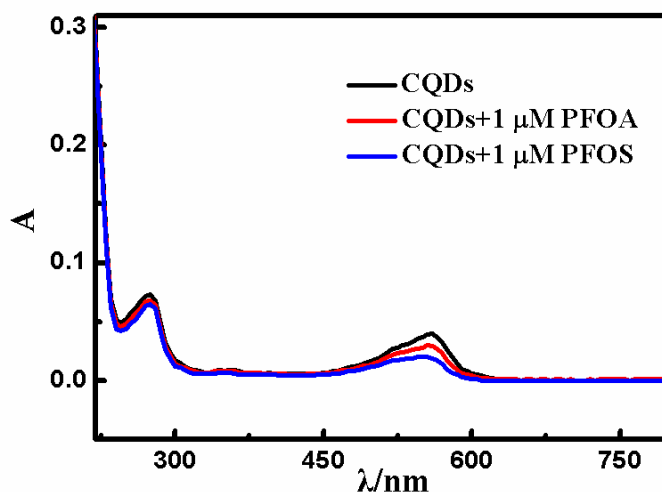


Fig. S9 UV-vis absorption spectra of CQDs and CQDs in the presence of 1 μM PFOS or PFOA

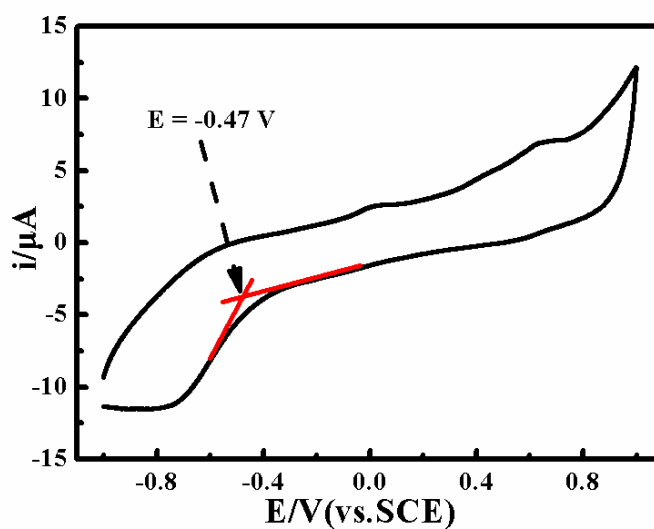


Fig. S10 Cyclic voltammograms of the CQDs dispersion in water

The HOMO and LUMO energy levels of CQDs were estimated from cyclic voltammetry results according to the empirical formula:

$$E_{\text{HOMO}} = -e(E_{\text{ox}} + 4.4)$$

$$E_{\text{LUMO}} = -e(E_{\text{red}} + 4.4)$$

Where E_{ox} and E_{red} are the onset of oxidation and reduction potential for CQDs,

respectively. The E_{red} was determined to be -0.47 V. The corresponding E_{LUMO} was calculated to be -3.93 eV. However, the HOMO energy could not be obtained from cyclic voltammetry due to the irreversibility of the oxidation behavior. To determine the HOMO levels, we combined the E_{red} with the optical band gap (E_{g} , from the absorbance spectrum):

$$E_{\text{HOMO}} = E_{\text{LUMO}} - E_{\text{g}}$$

E_{g} was estimated to be 1.98 eV, which leads to an E_{HOMO} value of -5.91 eV.

Table S2. Zeta potentials of CQDs in water at various pH

pH	Zeta potential (mV)
1.81	+15.3
2.21	+13.8
3.23	+11.4
4.10	+9.13
5.02	+8.05
6.09	+7.65
7.00	+6.99
8.36	+3.63
9.25	+0.124
10.38	-8.21

c_{CQDs} , 10 $\mu\text{g/mL}$ in BR buffer.

REFERENCES

- [1] J. Liu, X. Wang, F. Ma, X. Yang, Y. Liu, X. Zhang, S. Guo, Z. Wang, S. Yang, R. Zhao, Atomic copper(I)-carbon nitride as a peroxidase-mimic catalyst for high selective detection of perfluorooctane sulfonate, *Chem. Eng. J.* 435 (2022) 134966. <https://doi.org/10.1016/j.cej.2022.134966>.
- [2] Q. Zhang, M. Liao, K. Xiao, K. Zhuang, W. Zheng, Z. Yao, A water-soluble fluorescence probe

- based on perylene diimide for rapid and selective detection of perfluorooctane sulfonate in 100% aqueous media, *Sensor Actuat B-Chem* 350 (2022) 130851. <https://doi.org/10.1016/j.snb.2021.130851>.
- [3] Z. Cheng, H. Dong, J. Liang, F. Zhang, X. Chen, L. Du, K. Tan, Highly selective fluorescent visual detection of perfluorooctane sulfonate via blue fluorescent carbon dots and berberine chloride hydrate, *Spectrochim. Acta. A. Mol. Biomol. Spectrosc.* 207 (2019) 262-269. <https://doi.org/10.1016/j.saa.2018.09.028>.
- [4] Q. Chen, P. Zhu, J. Xiong, L. Gao, K. Tan, A new dual-recognition strategy for hybrid ratiometric and ratiometric sensing perfluorooctane sulfonic acid based on high fluorescent carbon dots with ethidium bromide, *SPECTROCHIM ACTA A* 224 (2020) 117362. <https://doi.org/10.1016/j.saa.2019.117362>.
- [5] Y. Wang, H. Zhu, Detection of PFOS and copper(ii) ions based on complexation induced fluorescence quenching of porphyrin molecules, *Anal. Methods* 6(7) (2014) 2379-2383. <https://doi.org/10.1039/c3ay41902a>.
- [6] J. He, Y. Su, Z. Sun, R. Zhang, F. Wu, Y. Bai, A chitosan-mediated "turn-on" strategy for rapid fluorometric detection of perfluorooctane sulfonate, *Microchem. J.* 157 (2020) 105030. <https://doi.org/10.1016/j.microc.2020.105030>.
- [7] L.S. Walekar, M. Zheng, L. Zheng, M. Long, Selenium and nitrogen co-doped carbon quantum dots as a fluorescent probe for perfluorooctanoic acid, *Mikrochim. Acta* 186(5) (2019) 278. <https://doi.org/10.1007/s00604-019-3400-2>.
- [8] Q. Liu, A. Huang, N. Wang, G. Zheng, L. Zhu, Rapid fluorometric determination of perfluorooctanoic acid by its quenching effect on the fluorescence of quantum dots, *J. Lumin.* 161 (2015) 374-381. <https://doi.org/10.1016/j.jlumin.2015.01.045>.
- [9] Z. Cheng, L. Du, P. Zhu, Q. Chen, K. Tan, An erythrosin B-based "turn on" fluorescent sensor for detecting perfluorooctane sulfonate and perfluorooctanoic acid in environmental water samples, *Spectrochim. Acta. A. Mol. Biomol. Spectrosc.* 201 (2018) 281-287. <https://doi.org/10.1016/j.saa.2018.05.013>.
- [10] L. Zheng, Y. Zheng, Y. Liu, S. Long, L. Du, J. Liang, C. Huang, M.T. Swihart, K. Tan, Core-shell quantum dots coated with molecularly imprinted polymer for selective photoluminescence sensing of perfluorooctanoic acid, *Talanta* 194 (2019) 1-6. <https://doi.org/10.1016/j.talanta.2018.09.106>.
- [11] W. Liu, S. Xu, Z. Li, R. Liang, M. Wei, D.G. Evans, X. Duan, Layer-by-Layer Assembly of Carbon Dots-Based Ultrathin Films with Enhanced Quantum Yield and Temperature Sensing Performance, *Chem. Mater.* 28(15) (2016) 5426-5431. <https://doi.org/10.1021/acs.chemmater.6b01792>.